IOP Publishing Phys. Scr. 98 (2023) 065905 https://doi.org/10.1088/1402-4896/acce7a

Physica Scripta

RECEIVED
15 February 2023

REVISED
5 April 2023

ACCEPTED FOR PUBLICATION
19 April 2023

PUBLISHED
28 April 2023

PAPER

# Structural and magnetic conduct in Sm and Al substituted $Ba_{0.9}Sm_{0.1}Fe_{10}Al_2O_{19}$ M-type hexaferrites at different sintering temperatures

**Basmah H Alshammari**[1], **Ubaid-ur-Rehman Ghori**[2], **Qasim Ali Ranjha**[3], **Sohail Ahmad**[4], **Waseem Abbas**[4], **Sana Ullah Asif**[5,*], **Fahim Ahmed**[6,*], **Fatma A Ibrahim**[7], **Mohamed S Hamdy**[7] **and Sayed M Eldin**[8]

[1] Chemistry Department, Faculty of Science, University of Hail, PO Box 2440, Hail 81451, Saudi Arabia
[2] Department of Industrial & Manufacturing Engineering (RCET), University of Engineering & Technology, Lahore, Pakistan
[3] Department of Mechanical Engineering, RCET Campus, University of Engineering and Technology, Lahore, Pakistan
[4] Institute of Physics, Bahauddin Zakariya University (BZU), Multan 60800, Pakistan
[5] Key Laboratory of LCR Materials and Devices of Yunnan Province, National Center for International Research on Photoelectric and Energy Materials, School of Materials and Energy, Yunnan University, Kunming 650091, People's Republic of China
[6] Department of Physics, Division of Science and Technology, University of Education, Lahore, Pakistan
[7] Catalysis Research Group (CRG), Department of Chemistry, College of Science, King Khalid University, PO Box 9004, Abha 61413, Saudi Arabia
[8] Center of Research, Faculty of Engineering, Future University in Egypt, New Cairo 11835, Egypt
[*] Authors to whom any correspondence should be addressed.

**E-mail:** sanaullahasif@gmail.com **and** Fahim.ahmed@ue.edu.pk

**Keywords:** M type hexaferrites, sintering temperature, x-ray diffraction, electron microscope, magnetic hysteresis loop, magnetic properties

## Abstract

The hexagonal ferrites with composition $Ba_{0.9}Sm_{0.1}Fe_{10}Al_2O_{19}$ has been prepared by using conventional solid state reaction method. As prepared samples were then sintered at different sintering temperatures to analyze the effects on magnetic and structural properties of Barium hexa ferrites. These samples were then characterized by using various techniques. For structural characterization x-ray diffraction technique was used. XRD results confirmed phase pure hexagonal structure. No impurity peaks were observed. For Morphological analysis of all the samples Scanning Electron Microscopy (SEM) was utilized. SEM micrographs suggested the formation of hexaferrites material with homogenous distribution of particles. Magnetic properties were measured by permanent magnetic measuring system. Magnetic conduction of material was tested under varying magnetic field of $\pm$ 30 KOe at room temperature. The saturation magnetization value was observed 48.55 emu $g^{-1}$ and coercivity 5.01KOe for the sample sintered at 1220 °C. As the sintering temperature rises, the values for magnetic saturation decreases to 46.24 emu $g^{-1}$ and coercivity increases up to 5.26 KOe at 1270 °C.

## 1. Introduction

M-type hexaferrites exhibit remarkable properties [1–3]. These materials are well known for their high chemical stability, resistance to corrosion, high electrical resistivity, high saturation magnetization, low cost and high Curie temperature [2, 4–6]. From the last few decades M type hexaferrites of Barium, Calcium, and, Strontium hexa ferrites are in considerable attention [6–12]. M-type hexa ferrites can be used as EMI shielding materials to reduce electromagnetic interference, as well as in microwave absorption device, magnetic recording media, and permanent magnets [4, 6–8, 11, 13–15]. M-type barium hexaferrite have general formula $BaFe_{12}O_{19}$ and is also referred as BaM [16]. Compared to their counter parts such as W-type Hexaferrites, U-type Hexaferrites, X-type Hexaferrites, Y-type Hexaferrites and Z-type Hexaferrites M-type Hexa ferrites have gained much attention owing to their superior magnetic traits [4–8].

Various synthesis routes have been proposed for the synthesis of M-type Hexaferrites [6]. Mostly used methods reported in literature are Ball Milling method [17], Co-precipitation route [18], Sol-Gel auto combustion route [19], Solid state synthesis method [20, 21], and hydrothermal method [22]. Comparison of these methods highlights Solid state synthesis method as more advantageous method and materials produced through this method showed high phase purity [23]. Also, solid state reaction method involves simple steps and provides more control over grain size of particles during synthesis [24]. Thereby, we also utilized solid state reaction method for synthesis of all the nominal samples in this research.

Literature review of M-type Hexaferrites materials confirmed that by carefully substituting various cations at $M^{2+}$ or $Fe^{3+}$ site their properties can be tailored further to achieve higher magnetic features. T. Kaur *et al* reported successful synthesis of Gd-Co substituted M-type barium hexaferrite, $Ba_{1-x}Gd_xCo_xFe_{12-x}O_{19}$, This research demonstrates that magnetic properties such as magnetization saturation and coercivity values were influenced by substitution of Gd-Co [25]. Chemical co-precipitation method was utilized by Habanjar *et al* to synthesize $BaFe_{12}O_{19}$ nanoparticles. Results shows coercivity ($H_c$) of the samples decreased after Co addition and was attributed to reduction in magnetocrystalline anisotropy [18]. In an another study M-type strontium calcium ferrite with the composition $Sr_{0.1}Ca_{0.4}La_{0.5}Fe_{12}O_{19}$ were prepared by utilizing solid-state reaction method. This study describes the effects of different precursors (Co-, Ni-, Cu-, Zn-, and Mg-type) on magnetic as well as on the structural properties [26]. Another way to alter the magnetic traits of hexagonal ferrites besides substitution is controlling the sintering temperature. Few studies published have shown the importance and effects of sintering temperature on magnetic and structural properties of Hexa ferrites [27, 28]. In our previous work we showed effects of different sintering temperature on magnetic properties of doped barium hexaferrites [29].

Here we report successful synthesis of M-type Hexaferrite with the nominal composition $Ba_{0.9}Sm_{0.1}Fe_{10}Al_2O_{19}$. For synthesis of all the samples we used solid state reaction method. To analyze sintering effects, we sintered synthesized sample at different temperatures. Structural analysis and morphological results confirmed the stability and phase dominance of material. Other micro parameters showed consistent behavior. Influence of variation in sintering temperature on the magnetic properties is discussed. The result suggests $Ba_{0.9}Sm_{0.1}Fe_{10}Al_2O_{19}$ hexaferrites can be a stable and economical material for magnetic applications in vast range of temperature.

## 2. Synthesis and characterizations

### 2.1. Material synthesis

Conventional solid state ceramic route was employed for synthesis. The stoichiometric amounts of starting raw materials $Fe_2O_3$ (Aldrich 99.9%), $BaCo_3$ (Aldrich 99.9%), $Al_2O_3$ (Aldrich 99.9%), and $Sm_2O_3$ (Aldrich 99.9 were taken and ball milled for 20 h in ethanol using steel jars. The resultant composition $Ba_{0.9}Sm_{0.1}Fe_{10}Al_2O_{19}$ were obtained by drying the ball milled solid solution. Furthermore, sintering of powder was carried out at different sintering temperatures from 1210 °C–1290 °C for 5 h in high temperature furnace. At the end, the material is used for further characterizations.

### 2.2. Characterization techniques

Field emission scanning electron microscopy (FE-SEM) (HITACHI S-4800) were used for morphological purposes. Structural measurements were carried out by Powder x-ray diffraction using Cu K$\alpha$ ($\lambda = 1.5406$ Å) radiation. Magnetic properties were measured by permanent magnetic measuring system (NIM-2000HF, China).

## 3. Results and discussions

### 3.1. Morphological analysis

Firstly, morphological studies of the $Ba_{0.9}Sm_{0.1}Fe_{10}Al_2O_{19}$ sintered at different temperatures were carried out by using scanning electron microscopy. The SEM micrographs suggested the formation of hexaferrites material with homogenous distribution of particles throughout the solid state solution. There is only a minor increase the grain size was observed with the increasing sintering temperature. SEM images also suggest that the material is free of secondary phases. However, at higher temperatures small agglomeration in the particles were found. Morphological images of the $Ba_{0.9}Sm_{0.1}Fe_{10}Al_2O_{19}$ were shown in figure 1. Furthermore, investigation on structure were carried out using x-ray diffraction analysis.

### 3.2. Structural investigations

The properties of the material strongly depend on the crystal structure and purity of the material [30]. Figure 2(a) illustrate the x-ray diffraction patterns of the $Ba_{0.9}Sm_{0.1}Fe_{10}Al_2O_{19}$ hexaferrites against different sintering temperatures. The diffraction peaks could be well matched with the hexagonal structure P63/mmc and

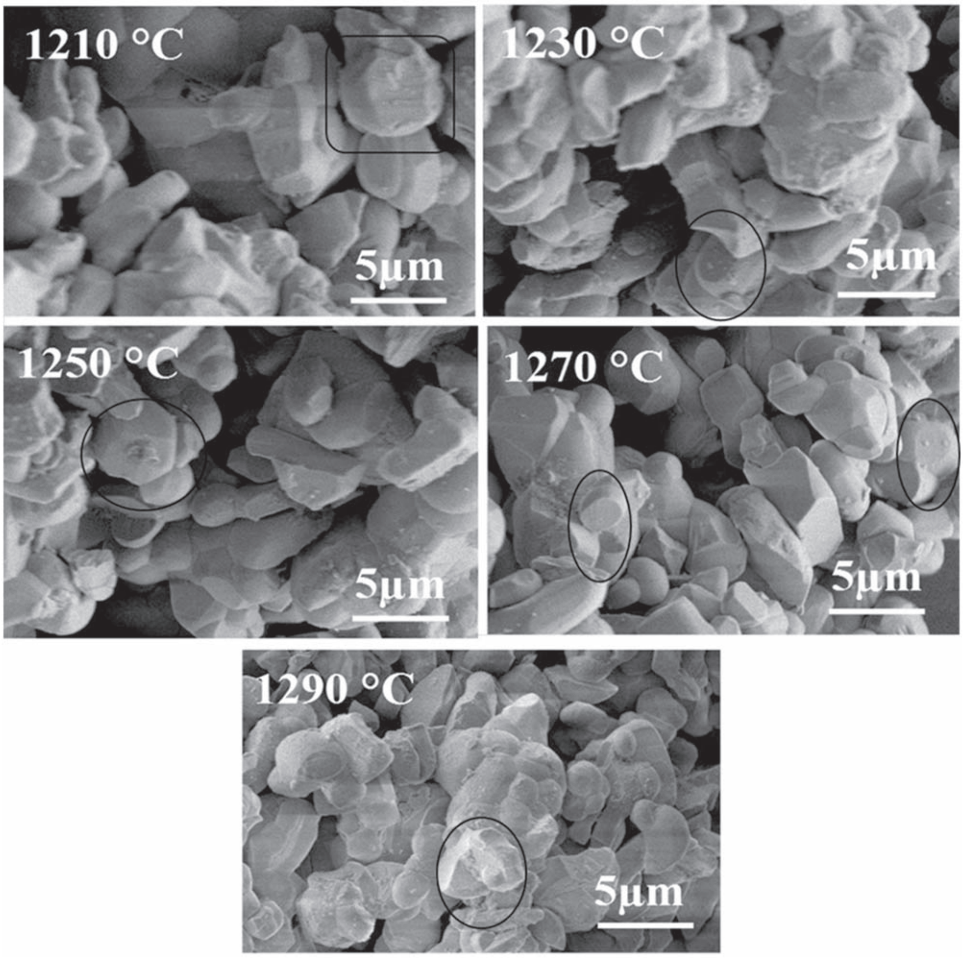


**Figure 1.** SEM images of $Ba_{0.9}Sm_{0.1}Fe_{10}Al_2O_{19}$ sintered at different temperatures.

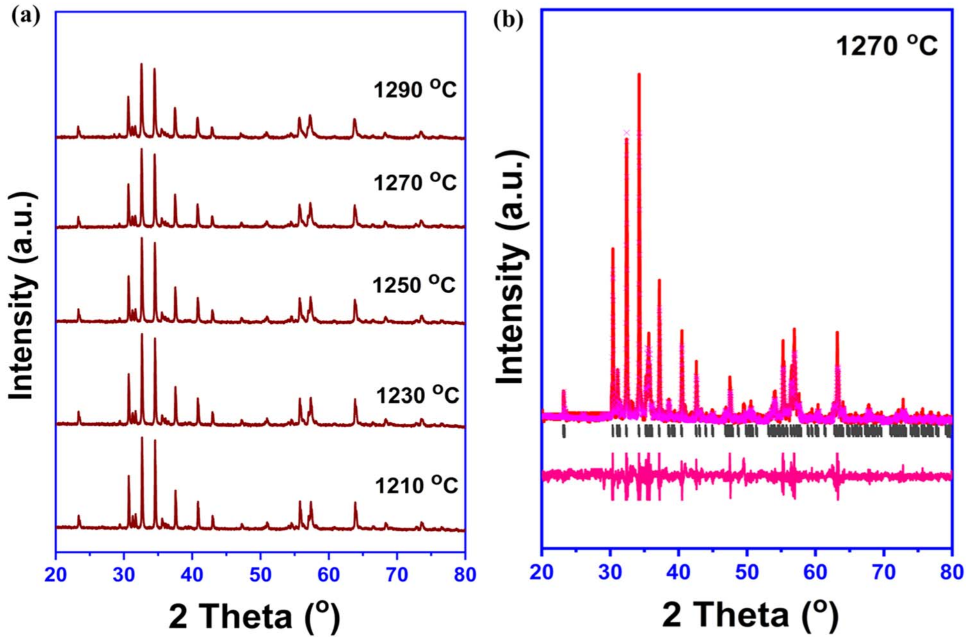


**Figure 2** (a)) XRD patterns of $Ba_{0.9}Sm_{0.1}Fe_{10}Al_2O_{19}$ sintered at different temperature. (b) Reitveld refinement profile of $Ba_{0.9}Sm_{0.1}Fe_{10}Al_2O_{19}$ sintered at 1270 °C. Red line represents the observed data, while Pink line represents the calculated fitting data. Red bottom line shows the difference along with black vertical symbols represents the Braggs peak position.

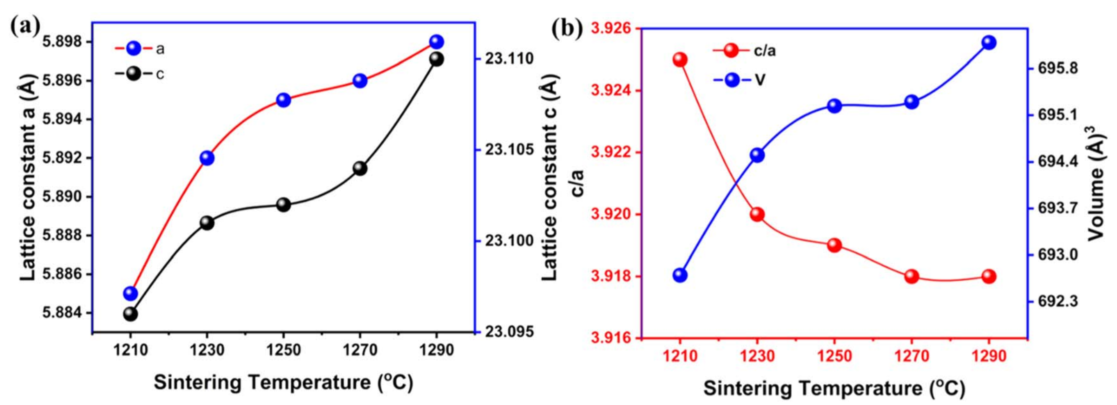


**Figure 3.** (a)) Lattice parameters of $Ba_{0.9}Sm_{0.1}Fe_{10}Al_2O_{19}$ sintered at different temperature. (b) Volume and the ratio(c/a) versus different temperatures.

follow the JCPDS#43-0002. The results showed minor change in the intensity also upon the introduction of dopant [31–33]. Lattice parameters were obtained using reitveld refinement analysis. Figure 2(b) showed the refinement profile of $Ba_{0.9}Sm_{0.1}Fe_{10}Al_2O_{19}$ hexaferrites against 1270 °C. The refinements were carried out using the main sites occupied by the Iron (Fe) including one trigonal bypyramidal site 2b, one tetrahedral site $4f_1$, and three more octahedral sites 2a, 12K and $4f_2$ respectively [34]. The calculate lattice parameters were shown in figures 3(a)–(b).

Lattice constant a and c both showed increasing trend with increasing sintering temperature confirming the expansion in longitudinal as well as along the *c*-axis at the same time. However, the increasing trend suggest the positive deviation of Vegard's Law [35, 36]. The expanding lattice of material with increasing temperature is quite interesting for the observation of magnetic outcomes. The formation of the M-type hexaferrites was further confirmed by calculating the c/a ratio for the material against different sintering temperature. The results below 3.98 is another indicator for the materials stability in the same M-type hexaferrites state through all temperatures. However, the changes in lattice dynamics suggest the strong influence of sintering temperature [37–41].

Furthermore, materials properties were further explored by investigating microstructure. Firstly, Bulk density($d_b$) and x-ray density ($d_x$) were calculated. Afterward Porosity (P) of the $Ba_{0.9}Sm_{0.1}Fe_{10}Al_2O_{19}$ sintered at different temperature were calculated from the diffraction data respectively. The average crystallite size was also measures by using Scherer method [42]. The crystallite size showed an increase with increase in sintering temperature and in agreement to morphological analysis. The formulas and equations used for calculations could be well studied from literature [43, 44].The obtained microstructural parameters were shown in figures 4(a)–(b). db and dx showed an increase with increasing sintering temperature, which could be weel-linked to the expansion of lattice with increasing temperature. X-ray density is greater than bulk density, suggesting the vacant sites as well as effective sintering temperature. This was further confirmed by calculation of dislocation density D from crystallite size [45, 46]. Normally as the temperature increases, sometimes it causes agglomeration and unification of crystallites, lead to dislocation in the crystal structure. Figure 4(b) clearly showed a overall decrease in porosity and dislocation of material as the sintering temperature increases. These variation in micro-parameters are co-related with the changes in the magnetic properties of material [47, 48].

### 3.3. Magnetic properties

Magnetic conduction of material was tested under varying magnetic field of ± 30 KOe at room temperature. Magnetic loops of hexaferrite $Ba_{0.9}Sm_{0.1}Fe_{10}Al_2O_{19}$ sintered at different temperatures, were shown in figure 5. The decrease in the magnetic saturation was observed with increasing temperature up to 1270 °C. However, is small rise in magnetic saturation was observed at 1290 °C. On the other hand, coercivity increases with increase in sintering temperature up to 1250 °C and started decreasing with further increase in sintering temperature. The obtained magnetic parameters were shown in figure 6. Magnetic remanance showed a comparative behavior like saturation magnetization. The saturation magnetization value was observed 48.55 emu $g^{-1}$ and coercivity 5.01KOe for the sample sintered at 1220 °C. As the sintering temperature rises, the values for magnetic saturation decreases to 46.24 emu $g^{-1}$ and coercivity increases up to 5.26 KOe at 1270 °C.

The values are quite comparable to the already reported values for undoped M-type hexaferrites. Somehow minor variations can be there and link to the synthesis conditions respectively [37, 43, 49–51]. Mr/Ms values are greater than 0.5 also indicate the existence of single anisotropy and domain structure of material [52, 53].

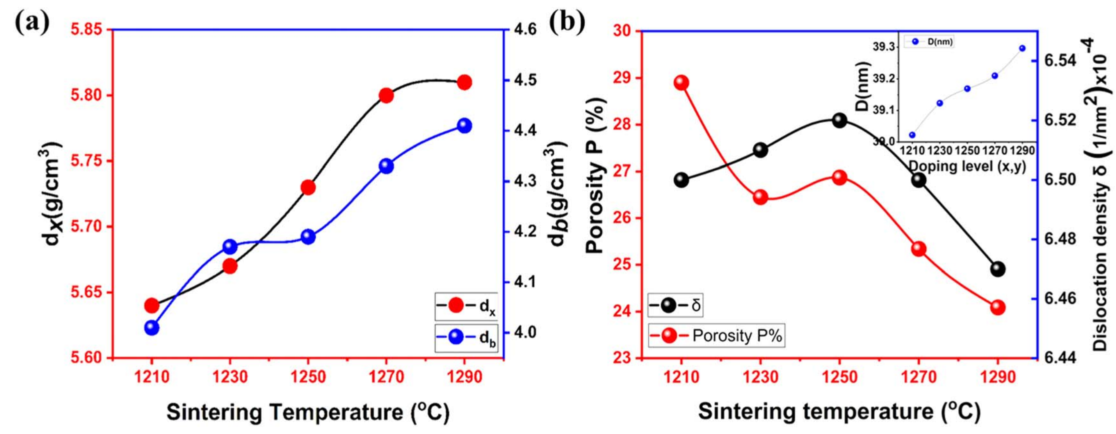


**Figure 4.** (a) Plots of $d_x$ and $d_b$ for different doping concentrations for $Ba_{0.9}Sm_{0.1}Fe_{10}Al_2O_{19}$ sintered at different temperatures. (b) Porosity and dislocation density versus sintering temperature. The inset shows variation of crystallite size (D) against sintering temperatures.

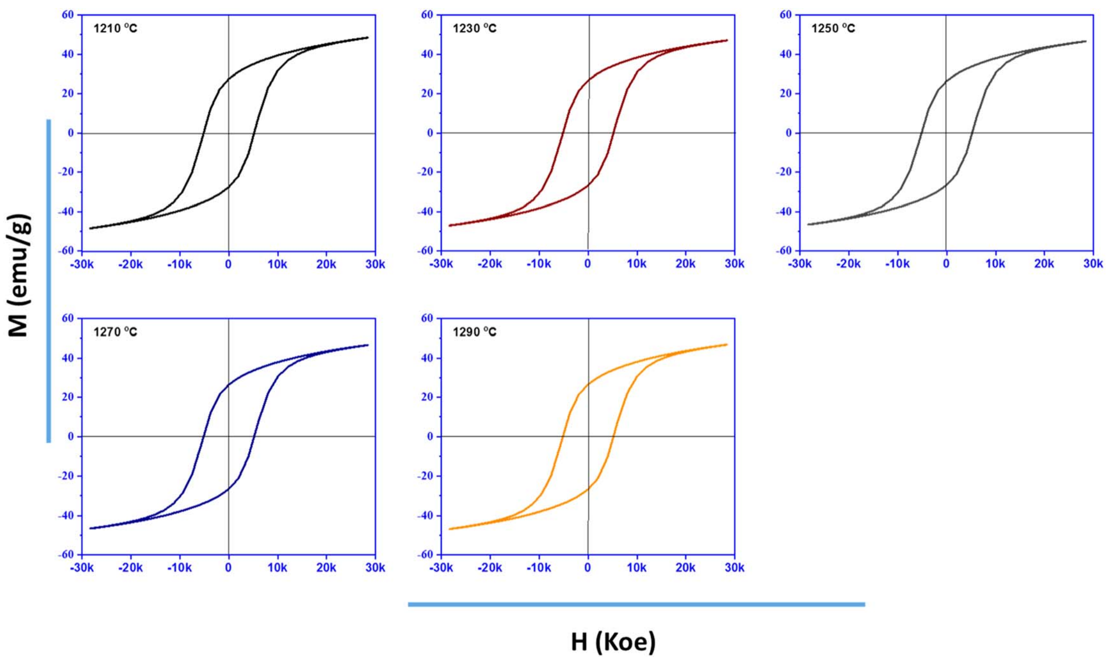


**Figure 5.** M-H loops for $Ba_{0.9}Sm_{0.1}Fe_{10}Al_2O_{19}$ sintered at different temperatures.

The variation in magnetic parameters may be due to the behavior of super exchange magnetic interactions disturbed by the sintering temperature [53–55]. Furthermore magnetic anisotropic constant K was found by using the Ms and Hc and shown in figure 6(c). Results showed That there is negligible change in the magnetic anisotropic constant K with the sintering temperature suggesting strong magnetic isotropic behaviour. However noteworthy and cyclic behavior of magnetic properties in material suggest that the material copiously well-suited with the common ferrite applications. The results also suggest that material is a good applicant under range of temperature for magnetic applications such as transformer and inductor cores, microwave devices, recording heads, and magnetic shielding.

## 4. Conclusions

M-type Hexaferrite $Ba_{0.9}Sm_{0.1}Fe_{10}Al_2O_{19}$ prepared by solid state reaction method and afterward sintered at different temperatures. Structural anaylsis and morphological results confirmed the stability and phase dominance of material. Other micro parameters showed consistent behaviour. Firstly, coercivity increases and magnetic saturation increased with increasing temperature. the maximum was observed at 1270 °C. No

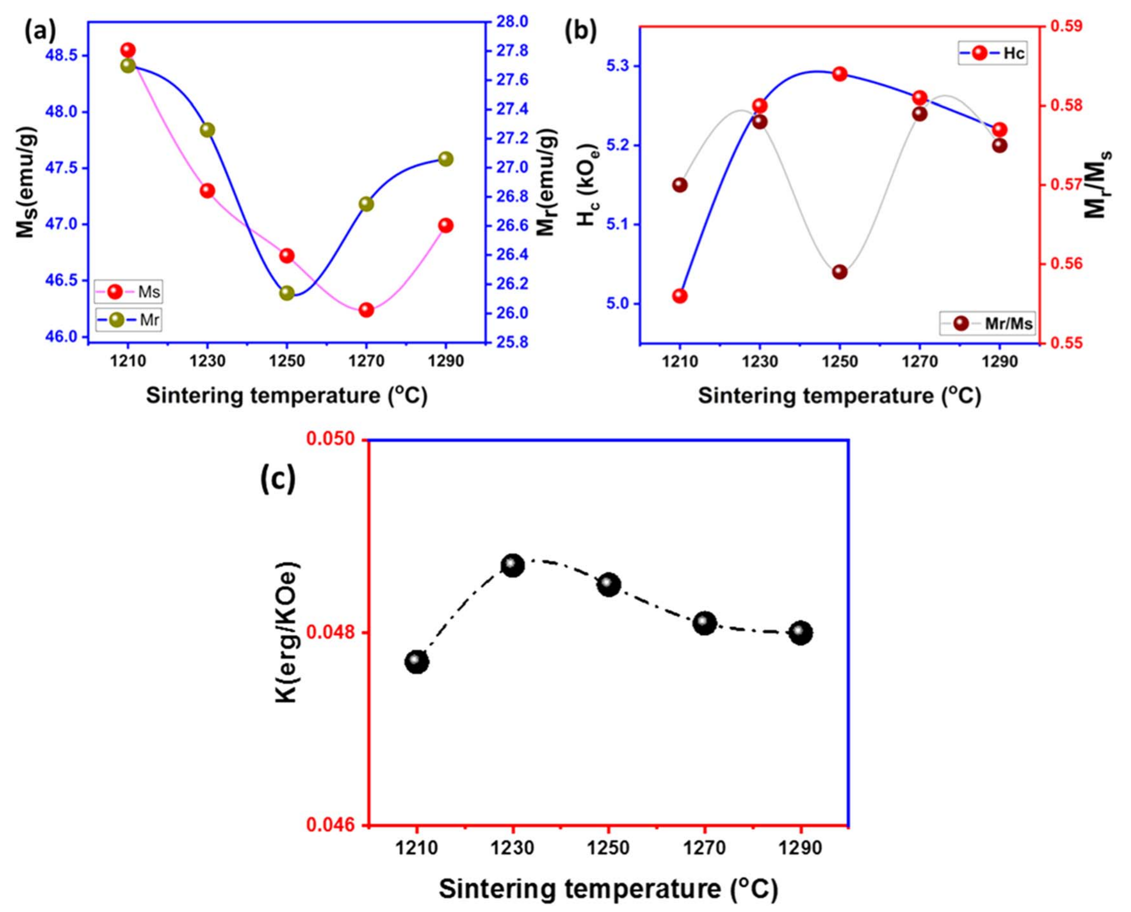


**Figure 6.** Plots of Ms and Mr for $Ba_{0.9}Sm_{0.1}Fe_{10}Al_2O_{19}$ sintered at different temperatures. (b) squareness ratio for $Ba_{0.9}Sm_{0.1}Fe_{10}Al_2O_{19}$ sintered at different temperatures. (c) Magnetic anisotropic constant K versus sintering temperature.

significant effects were observed for magnetic anisotropic constant k. The trend shifted toward opposite above this temperature. The result suggests $Ba_{0.9}Sm_{0.1}Fe_{10}Al_2O_{19}$ hexaferrites can be a stable and economical material for magnetic applications in vast range of temperature.

## Acknowledgments

The authors are thankful to the Deanship of Scientific Research at King Khalid University for funding this work through a large group Research Project under grant number RGP2/236/44.

## Data availability statement

All the data included in the manuscript and available from authors on request. The data that support the findings of this study are available upon reasonable request from the authors.

## Author contributions

All the authors contributed equally in this work. All the authors analyzed the data. The manuscript was written through the contributions of all authors. All authors have given approval to the final version of the manuscript.

## Declaration

The authors declare that they have no known competing financial interests or personal relationships that could have appeared to influence the work reported in this paper.

## ORCID iDs

Basmah H Alshammari https://orcid.org/0000-0002-5876-3700
Sana Ullah Asif https://orcid.org/0000-0002-1521-5747
Mohamed S Hamdy https://orcid.org/0000-0002-7234-4924
Sayed M Eldin https://orcid.org/0000-0002-0229-0705

## References

[1] Zahid M, Siddique S, Anum R, Shakir M F, Nawab Y and Rehan Z A 2021 M-Type Barium Hexaferrite-Based Nanocomposites for EMI shielding application: a review *J. Supercond. Nov. Magn.* **34** 1019–45
[2] Cochardt A 1966 Recent ferrite magnet developments. *J. Appl. Phys.* **37** 1112–5
[3] Cullity B D and Graham C D 2011 *Introduction to Magnetic Materials* 2nd edn (New York: Wiley) (https://doi.org/10.1002/9780470386323)
[4] Dairy A R A, Al-Hmoud L A and Khatatbeh H A 2019 Magnetic and structural properties of barium hexaferrite nanoparticles doped with titanium *Symmetry* **11** 732
[5] Narang S B and Pubby K 2021 Nickel spinel ferrites: a review *J. Magn. Magn. Mater.* **519** 167163
[6] Pullar R C 2012 Hexagonal ferrites: a review of the synthesis, properties and applications of hexaferrite ceramics *Prog. Mater Sci.* **57** 1191–334
[7] Anjum S, Hameed S, Awan M S, Amed E and Sattar A 2017 Effect of strontium doped M-Type bariam hexa-ferrites on structural, magnetic and optical properties *Optik* **131** 977–85
[8] Bielan Z, Dudziak S, Kubiak A and Kowalska E 2021 Application of spinel and hexagonal ferrites in heterogeneous photocatalysis **11** 10160
[9] González-Angeles A, Mendoza-Suárez G, Grusková A, Tóth I, Jančárik V, Papánová M and Escalante G 2004 Magnetic studies of NiSn-substituted barium hexaferrites processed by attrition milling *J. Magn. Magn. Mater.* **270** 77–83
[10] Hessien M M, Turky A O, Alanazi A K, Alsawat M, Mahmoud M H H, El-Bagoury N and Rashad M 2021 Boost the crystal installation and magnetic features of Cobalt Ferrite/M-Type strontium ferrite nanocomposites double substituted by La3+ and Sm3+ Ions (2CoFe2O4/SrFe12−2xSmxLaxO19) *Materials* **14** 7820
[11] Khan H M, Islam M U, Xu Y, Naeem Ashiq M, Ali I, Asif Iqbal M and Ishaque M 2014 Structural and magnetic properties of Pr–Ni substituted Ca0.5Ba0.5Fe12O19 hexa-ferrite nanoparticles *Ceram. Int.* **40** 6487–93
[12] Yasmin N, Yasmin S, Zahid M, Gillani S F, Islam M U, Altaf M, Khan H M, Safdar M and Mirza M 2020 Impact of Ho-Ni substitution on structural, morphological and dielectrical characteristics of BaFe12O19 M-type hexagonal ferrite *Physica* **581** 411950
[13] Ginting M, Sebayang P, Rianna M, Situmorang M, Fujiati H, Tetuko A P, Setiadi E A, Kurniawan C and Sebayang A M S 2020 Effect of Co and Ni additions as doping materials on the micro-structures and the magnetic properties of barium hexa-ferrites *Case Studies in Thermal Engineering* **18** 100589
[14] Khan M A, Qamar uz Zaman M, Majeed A, Akhtar M N and Abbas W 2021 Structural, spectral, dielectric and magnetic properties of Sr2CuxNi2-xFe28-xCrxO46 ($0 \leqslant x \geqslant 0.5$) ferrites synthesized via micro-emulsion route *Mater. Chem. Phys.* **259** 124066
[15] Niu X, Liu X, Feng S, Lv F, Huang F, Huang X, Ma Y and Huang K 2015 Effects of presintering temperature on structural and magnetic properties of BaMg1.8Cu0.2Fe16O27 hexagonal ferrites *Optik* **126** 5513–6
[16] Maswadeh Y, Mahmood S H, Awadallah A and Aloqaily A N 2015 Synthesis and structural characterization of nonstoichiometric barium hexaferrite materials with Fe:Ba ratio of 11.5—16.16 *IOP Conf. Ser.: Mater. Sci. Eng.* **92** 012019
[17] Chen D, Harward I, Baptist J, Goldman S and Celinski Z 2015 Curie temperature and magnetic properties of aluminum doped barium ferrite particles prepared by ball mill method *J. Magn. Magn. Mater.* **395** 350–3
[18] Habanjar K, Shehabi H, Abdallah A M and Awad R 2020 Effect of calcination temperature and cobalt addition on structural, optical and magnetic properties of barium hexaferrite BaFe12O19 nanoparticles *Appl. Phys.* **126** 402
[19] Godara S K, Kaur V, Narang S B, Singh G, Singh M, Bhadu G R, Chaudhari J C, Babu P D and Sood A K 2021 Tailoring the magnetic properties of M-type strontium ferrite with synergistic effect of co-substitution and calcinations temperature *Journal of Asian Ceramic Societies* **9** 686–98
[20] Hussain S and Maqsood A 2007 Influence of sintering time on structural, magnetic and electrical properties of Si–Ca added Sr-hexa ferrites *J. Magn. Magn. Mater.* **316** 73–80
[21] Rafiq M A, Waqar M, Mirza T A, Farooq A and Zulfiqar A 2017 Effect of Ni2+ Substitution on the structural, magnetic, and dielectric properties of barium hexagonal ferrites (BaFe12O19) *J. Electron. Mater.* **46** 241–6
[22] Xia A, Zuo C, Chen L, Jin C and Lv Y 2013 Hexagonal SrFe12O19 ferrites: Hydrothermal synthesis and their sintering properties *J. Magn. Magn. Mater.* **332** 186–91
[23] Yang Y, Wang F, Shao J, Huang D, Trukhanov A V and Trukhanov S V 2018 Preparation of Al3+-Co2+ co-substituted M-type SrCaNd hexaferrites and their controlled magnetic properties *AIP Adv.* **8** 075212
[24] Yang Y, Chen C, Chen D, Zhang Y, Meng Y, Zhang C and Feng S 2022 Investigation into the structural, spectral, magnetic, and electrical properties of cobalt-substituted strontium W-Type hexaferrites *Magnetochemistry* **8** 75
[25] Kaur T, Sharma J, Kumar S and Srivastava A K 2017 Optical and multiferroic properties of Gd-Co substituted Barium hexaferrite *Cryst. Res. Technol.* **52** 1700098
[26] Zhao X, Zhang S, Li J, Xia A and Yang Y 2022 Microstructure and magnetic properties of M-Type Sr0.1Ca0.4La0.5Fe12O19 ferrites: the impact of different precursors *Magnetochemistry* **8** 68
[27] Ahmad M, Ali I, Aen F, Islam M U, Ashiq M N, Atiq S, Ahmad W and Rana M U 2012 Effect of sintering temperature on magnetic and electrical properties of nano-sized Co2W hexaferrites *Ceram. Int.* **38** 1267–73
[28] Moon K-S, Yu P-y and Kang Y-M 2020 Microstructure and magnetic properties of La-Ca-Co substituted M-Type Sr-Hexaferrites with controlled Si diffusion *applied sciences* **10** 7570
[29] Makhdoom A R *et al* 2021 Structural and magnetic variations in Ba0.5Sr0.5Fe9Ce1Al2O19 hexaferrites at different sintering temperatures *Phys. Scr.* **96** 125865
[30] Asif S U, Wang J, Qian Y, Gao D, Bashir R, Bilal M K, Ahmad J, Awan M Q and Hu W 2020 Phonon vibrations and photoluminescence emissions and their correlations with the electrical properties in Er3+ doped Bi3YO6 oxide-ion conductors *Solid State Ionics* **344** 115092

[31] Alsmadi A M, Bsoul I, Mahmood S H, Alnawashi G, Al-Dweri F M, Maswadeh Y and Welp U 2015 Magnetic study of M-type Ru–Ti doped strontium hexaferrite nanocrystalline particles *J. Alloys Compd.* **648** 419–27

[32] Makhdoom A R *et al* 2021 Structural and magnetic variations in Ba0.5Sr0.5Fe9Ce1Al2O19 hexaferrites at different sintering temperatures *Phys. Scr.* **96** 125865

[33] Makhdoom A R *et al* 2022 Tuning magnetic properties in the Ce–Al Co-substituted M-type BaSr (6:4) hexaferrites *Journal of Materials Science: Materials in Electronics* **33** 7266–74

[34] Trusov L A, Gorbachev E A, Lebedev V A, Sleptsova A E, Roslyakov I V, Kozlyakova E S, Vasiliev A V, Dinnebier R E, Jansen M and Kazin P E 2018 Ca–Al double-substituted strontium hexaferrites with giant coercivity *Chem. Commun.* **54** 479–82

[35] Denton A R and Ashcroft N W 1991 Vegard's law *Phys. Rev.* **43** 3161–4

[36] Petkov V, Maswadeh Y, Vargas J A, Shan S, Kareem H, Wu Z-P, Luo J, Zhong C-J, Shastri S and Kenesei P 2019 Deviations from Vegard's law and evolution of the electrocatalytic activity and stability of Pt-based nanoalloys inside fuel cells by in operando x-ray spectroscopy and total scattering *Nanoscale* **11** 5512–25

[37] Rehman K M U, Liu X, Li M, Jiang S, Wu Y, Zhang C, Liu C, Meng X and Li H 2017 Synthesization and magnetic properties of Ba1−xYxFe12O19 hexaferrites prepared by solid-state reaction method *J. Magn. Magn. Mater.* **426** 183–7

[38] Liu C *et al* 2019 Investigations of Ce-Zn co-substitution on crystal structure and ferrimagnetic properties of M-type strontium hexaferrites Sr1-xCexFe12-xZnxO19 compounds *J. Alloys Compd.* **785** 452–9

[39] Mathews S A and Babu D R 2021 Analysis of the role of M-type hexaferrite-based materials in electromagnetic interference shielding *Current Applied Physics* **29** 39–53

[40] Khan S, Ahmed I, Khalid N, Mehmood M, Waheed A and Malik M 2015 Carbon ions irradiation induced modifications in structural and electrical resistivity characteristics of ZrN thin films *Mater. Sci. Semicond. Process.* **39** 530–5

[41] Shezad M, Liu X, Feng S, Kan X, Wang W, Liu C, Shehzad T J and Rehman K M U 2020 Characterizations analysis of magneto-structural transitions in Ce-Co doped SrM based nano Sr1− xCexFe12− xCoxO19 hexaferrite crystallites prepared by ceramic route *J. Magn. Magn. Mater.* **497** 166013

[42] Bindu P and Thomas S 2014 Estimation of lattice strain in ZnO nanoparticles: x-ray peak profile analysis *Journal of Theoretical and Applied Physics* **8** 123–34

[43] Makhdoom A R *et al* 2022 Tuning magnetic properties in the Ce–Al Co-substituted M-type BaSr (6:4) hexaferrites *J. Mater. Sci., Mater. Electron.* **33** 7266–74

[44] Asif S U *et al* 2019 Effect of Dy-Co on physical and magnetic properties of X-type hexaferrites (Ba2−xDyxCu2Fe28−yCoyO46) *Chin. J. Phys.* **61** 47–54

[45] Hoffman R W 1981 Stress distributions and thin film mechanical properties *Surf. Interface Anal.* **3** 62–6

[46] Vlassak J 2004 A model for chemical–mechanical polishing of a material surface based on contact mechanics *J. Mech. Phys. Solids* **52** 847–73

[47] Deraz N and Alarifi A 2012 Processing and evaluation of alumina doped nickel ferrite nano-particles *Int. J. Electrochem. Sci.* **7** 4585–95

[48] Verma A, Thakur O, Prakash C, Goel T and Mendiratta R 2005 Temperature dependence of electrical properties of nickel–zinc ferrites processed by the citrate precursor technique *Materials Science and Engineering:* B **116** 1–6

[49] Pereira F M M, Santos M R P, Sohn R S T M, Almeida J S, Medeiros A M L, Costa M M and Sombra A S B 2009 Magnetic and dielectric properties of the M-type barium strontium hexaferrite (BaxSr1−xFe12O19) in the RF and microwave (MW) frequency range *J. Mater. Sci., Mater. Electron.* **20** 408–17

[50] Pereira F M M, Junior C, Santos M R P, Sohn R S T M, Freire F N A, Sasaki J M, De Paiva J and Sombra A S B 2008 Structural and dielectric spectroscopy studies of the M-type barium strontium hexaferrite alloys (Ba x Sr 1− x Fe 12 O 19) *J. Mater. Sci., Mater. Electron.* **19** 627–38

[51] Ahmad J, Makhdoom A R, Sabir M, Asif S U and Awan M Q 2019 Electrical transport properties of cobalt-doped MgAl2O4 nanoparticles *Phys. Scr.* **94** 105814

[52] Stoner E C and Wohlfarth E P 1948 A mechanism of magnetic hysteresis in heterogeneous alloys *IEEE Trans Magnetics* **27** 3475–518

[53] Bobade D H, Rathod S M and Mane M L 2012 Sol–gel auto-combustion synthesis, structural and enhanced magnetic properties of Ni2+ substituted nanocrystalline Mg–Zn spinel ferrite *Physica* **407** 3700–4

[54] Slimani Y, Baykal A, Amir M, Tashkandi N, Güngüneş H, Guner S, El Sayed H, Aldakheel F, Saleh T A and Manikandan A 2018 Substitution effect of Cr3+ on hyperfine interactions, magnetic and optical properties of Sr-hexaferrites *Ceram. Int.* **44** 15995–6004

[55] Almessiere M, Slimani Y and Baykal A 2018 Structural and magnetic properties of Ce-doped strontium hexaferrite *Ceram. Int.* **44** 9000–8